

Synthesis, structural characterization and *in vitro* inhibitory studies against human breast cancer of the bis-(2,6-di-*tert*-butylphenol)tin(IV) dichloride and its complexes†

D. B. Shpakovsky,^{a,b} C. N. Banti,^{a,c} G. Beaulieu-Houle,^{a,d} N. Kourkoumelis,^e M. Manoli,^f M. J. Manos,^f A. J. Tasiopoulos,^f S. K. Hadjikakou,^{*a} E. R. Milaeva,^b K. Charalabopoulos,^{c,g} T. Bakas,^h I. S. Butler^d and N. Hadjiliadis^a

Received 11th July 2012, Accepted 14th September 2012

DOI: 10.1039/c2dt31527k

Four new organotin(IV) complexes of bis-(2,6-di-*tert*-butylphenol)tin(IV) dichloride [$(\text{tert-Bu})_2(\text{HO-Ph})_2\text{SnCl}_2$ (**1**) with the heterocyclic thioamides 2-mercapto-pyrimidine (PMTH), 2-mercapto-4-methyl-pyrimidine (MPMTH), 2-mercapto-pyridine (PYTH) and 2-mercapto-benzothiazole (MBZTH), of formulae $\{[(\text{tert-Bu})_2(\text{HO-Ph})_2\text{Sn}(\text{PMT})_2\}$ (**2**), $\{[(\text{tert-Bu})_2(\text{HO-Ph})_2\text{Sn}(\text{MPMT})_2\}$ (**3**), $\{[(\text{tert-Bu})_2(\text{HO-Ph})_2\text{SnCl}(\text{PYT})\}$ (**4**) and $\{[(\text{tert-Bu})_2(\text{HO-Ph})_2\text{SnCl}(\text{MBZT})\}$ (**5**), have been synthesized and characterized by elemental analysis, ^1H -, ^{13}C -, ^{119}Sn -NMR, EPR, FT-IR, Raman and Mössbauer spectroscopic techniques. The crystal and molecular structures of compounds **1–5** have been determined by X-ray diffraction. The geometries around the metal center adopted in complexes **1–5** varied between tetrahedral in **1**, trigonal bipyramidal in **3**, **4**, **5** and distorted octahedral in **2**. Two carbon atoms from aryl groups and two chlorine atoms form a distorted tetrahedron in the case of **1**. Two carbon, two sulfur and two nitrogen atoms from thione ligands form a distorted octahedral geometry around tin(IV) with *trans*- C_2 , *cis*- N_2 , *cis*- S_2 -configurations in **2**. However, in the case of **4** and **5** complexes two carbon, one sulfur, one nitrogen and one chloride atom form a distorted trigonal bipyramidal arrangement. Finally, in the case of **3** the trigonal bipyramidal geometry is achieved by two carbon, two sulfur and one nitrogen atom in a unique coordination mode of thioamides toward the tin(IV) cation. Compounds **1–5** were tested for their *in vitro* cytotoxicity against the human breast adenocarcinoma (MCF-7) cell line. Compound **3** exhibits strong cytotoxic activity against MCF-7 cells ($\text{IC}_{50} = 0.58 \pm 0.1 \mu\text{M}$).

1. Introduction

Organotin compounds are widely used as agricultural and industrial biocides due to their antifungal properties.¹ The intensive study of organotin compounds had begun after the discovery of their anti-tumor activity by M. Gielen in the 1980s.^{2,3} The mechanism of anti-tumour activity is still under investigation.⁴ It is well known that the Sn-atom interacts with free sulfhydryl groups in proteins leading to distortion of the protein structure. The thymotoxic di-*n*-butyltin dichloride and tri-*n*-butyltin chloride affect macromolecular DNA synthesis in rat thymocytes *in vivo*.⁵ Organotin complexes with heterocyclic thioamides demonstrated high antiproliferative activity which was correlated to the lipoxigenase (LOX) inhibiting activity by depleting HS-groups in proteins which are restricted when the organotin complexes possess the S-bonded ligands.⁶ The inhibition activity of tin–thioamide complexes was found to be influenced by the nature of the ligand to a great extent.^{6,7}

Organotin(IV) complexes with ligands containing phenolic –OH groups and heterocyclic nitrogen donor atoms, *e.g.* 4,6-dihydropyrimidine or 2-thiobarbituric acid, represent a peculiar class due to their ability to form the phenoxyl radical

^aSection of Inorganic and Analytical Chemistry, Department of Chemistry, University of Ioannina, 45110 Ioannina, Greece.

E-mail: shadjika@uoi.gr; Fax: +30-26510-08786;

Tel: +30-26510-08374

^bChemistry Department Moscow State Lomonosov University, Moscow, Russian Federation

^cDepartment of Experimental Physiology, Medical School, University of Ioannina, Greece

^dDepartment of Chemistry, McGill University, 801 Sherbrooke, Montreal, Quebec, Canada

^eMedical Physics Laboratory, Medical School, University of Ioannina, Ioannina, Greece

^fDepartment of Chemistry, University of Cyprus, 1678 Nicosia, Cyprus

^gDepartment of Physiology, Democritus University Medical School, Greece

^hPhysics of Material Laboratory, Department of Physics, University of Ioannina, Greece

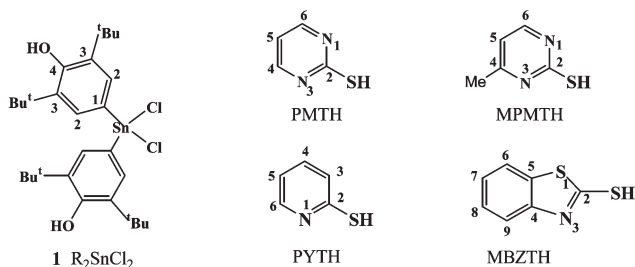
† Electronic supplementary information (ESI) available. CCDC 891289 (**1**), 891290 (**2**), 891291 (**3**), 891292 (**4**) and 891293 (**5**). For ESI and crystallographic data in CIF or other electronic format see DOI: 10.1039/c2dt31527k

during oxidation.^{7,8} These complexes were synthesized by refluxing a methanol solution of the sodium salt of the ligands with organotin halides. The complexes of tri-*n*-butyltin(IV) and triphenyltin(IV) with 2-thiobarbituric acid, [(*n*-Bu)₃Sn(O-HTBA)·H₂O] and {[Ph₃Sn(O-HTBA)·0.7H₂O]}_n,⁷ were found to exhibit better cytotoxic activity than that of cisplatin against cancer cells, which in the case of breast cancer cells (MCF-7) (ER positive) their IC₅₀ values were 272 and 179-fold lower than that of cisplatin respectively.^{7a}

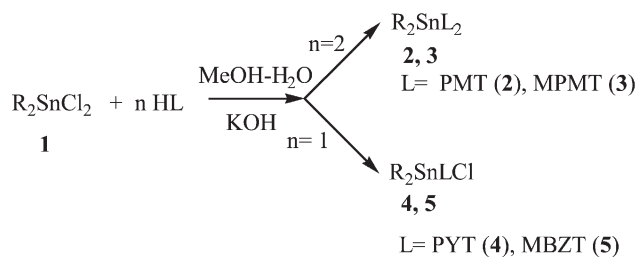
Breast cancer, on the other hand, is the most prevalent cancer in the world today, because of its high incidence and relatively good prognosis.^{9a} It is estimated that 4.4 million women alive have breast cancer diagnosed within the last 5 years and the incidence rates are increasing.^{9a} The MCF-7 cell line has been previously used as a model for human breast cancer.^{9b} Recently, Kobakhidze *et al.*^{9c} reported that di-*n*-butyltin(IV) or diphenyltin(IV) complexes with the Schiff bases which derived from α-amino acids (isoleucine, leucine, methionine, phenylalanine and aminophenylacetic acid) with aldehydes (2,4-dihydroxybenzaldehyde, 2-hydroxy-4-methoxybenzaldehyde) exhibited selective activity against MCF-7 cells.^{9c} Complexes {[Ph₃Sn(O-HTBA)·0.7H₂O]}_n and [(*n*-Bu)₃Sn(O-HTBA)·H₂O]}_n^{7a} also showed selective activity against MCF-7. This strong selective activity of [(*n*-Bu)₃Sn(O-HTBA)·H₂O]}_n and {[Ph₃Sn(O-HTBA)·0.7H₂O]}_n⁷ complexes against MCF-7 (ER positive) was not observed when they were tested against breast cancer cells (MDA-MB-231) (breast, ER negative), indicating that estrogen receptors (ER) may be involved in their antitumor mechanism.^{7a} It is also reported that antiestrogen drugs such as tamoxifen inhibit the growth of MCF-7 cells by blocking the steroid receptors (ER-α and ER-β) which are located in human breast cancer cells,^{9d,e} since estrogen receptors are expressed in human breast cancer.^{9f} Therefore, this sex steroid plays an important role in the development and propagation of the disease.^{9f}

The organic derivatives of hindered 2,6-di-alkylphenols are considered as synthetic antioxidants and models of vitamin E.¹⁰ Metal complexes bearing antioxidative groups of 2,6-di-*tert*-butylphenols act as polyfunctional antioxidants, anti-inflammatory agents, and scavengers for reactive oxygen species¹¹ which make them promising agents in cancer therapy.

In the present paper, we report on the synthesis and characterization of diorganotin complexes with the 2,6-di-*tert*-butylphenol moiety with various thioamides and aromatic thiols (Scheme 1). The X-ray crystal structures of the complexes are described herein. The *in vitro* anti-tumor activity of the complexes against the human breast adenocarcinoma (MCF-7) tumor cell line is also studied.



Scheme 1 Molecular formulae of di-organotin dichloride and ligands used in this work.



Scheme 2 Reactions for the preparation of 2–5.

Results and discussion

General aspects

The synthesis of R₂SnCl₂ (**1**) was carried out by the re-metallation reaction of RHgCl and Sn in *o*-xylene under reflux according to a previously reported method.¹² Organotin(IV) complexes **2–5** have been synthesized by reacting a methanolic solution of organotin dichloride R₂SnCl₂ (**1**) with an aqueous solution of the appropriate ligand (thioamides) containing an equivalent amount of potassium hydroxide as shown in Scheme 2.

Compounds **1–5** are stable in air and in solution. Crystals suitable for X-ray analysis were obtained by slow evaporation of methanol–acetonitrile solutions (1 : 1) for compounds **2**, **4** or by slow diffusion of hexane in chloroform solution in the case of **3**, **5**. Crystals of **1** were obtained by slow evaporation of an *o*-xylene solution.

Spectroscopy

(a) Vibrational spectroscopy. Characteristic infrared bands of the complexes and the ligands are presented in Table 1 (Fig. S1–S5†). The IR spectra of **1–5** in KBr feature characteristic narrow absorptions in the region of 3595–3640 cm⁻¹ which was assigned to the free hindered phenol group. Complexes **4**, **5** with *S*-substituted pyridine and benzothiazole also demonstrate another wide band at 3440–3420 cm⁻¹ related to hydrogen bond formation between the phenol group and the neighboring pyridine and carboxylate moiety of the complex molecule that is nontrivial for hindered phenols. The IR spectra of the complexes also show distinct vibrational bands at 1595–1420 and 1320–1240 cm⁻¹, which can be assigned to ν(C=N) vibrations of thioamide (I and II bands), and at 1100–1005 and 950–640 cm⁻¹, which can be attributed to the ν(CS) vibrations (thioamide III and IV bands). No bands due to the ν(NH) or ν(SH) vibrations are observed in the IR spectra of the complexes, indicating the de-protonation of all ligands. Significant changes between the IR spectra of the ligands and the complexes were also observed (Table 1). Thioamide bands are shifted to lower frequencies in the spectra of the complexes, supporting sulfur donation and de-protonation of the ligands as well. Bands at 580–560 cm⁻¹ have been assigned to the anti-symmetric and symmetric vibrations of the Sn–C bond while the bands at 375–385 cm⁻¹ are attributed to the ν(Sn–S) vibrations.^{6,7,13} Sn–S and Sn–N vibrations are also Raman active.^{6d} Thus, the bands at 240–270 cm⁻¹ in the Raman spectra of complexes **1–5** are due to ν(Sn–N), whereas those at 340–390 cm⁻¹ are assigned to ν(Sn–S) (Table 1)^{6d} (Fig. S6–S9†).

Table 1 Characteristic vibration bands (cm^{-1}) in the infrared and Raman spectra of complexes and ligands

Compound	Infrared							Raman	
	$\nu(\text{NH})$, $\nu(\text{OH})$	$\nu(\text{CH})$	Thioamide I	Thioamide II	Thioamide III	Thioamide IV	$\nu(\text{Sn}-\text{C})$	$\nu(\text{Sn}-\text{S})$	$\nu(\text{Sn}-\text{N})$
1	3614	2963–2872	1427 s	1241	1120	874	568 w	—	—
PMTH	3468	3054–2930	1439	1256	1054	984	—	—	—
2	3420	2872–2965	1427	1220	1121	989	575	399	238
MPMTH HCl	3440	3074	1463	1234	1003	916	—	—	—
3	3636, 3449 br	2877–2958	1430	1239	1025	885	573	333	251
PYTH	3163	3050–2800	1496, 1439	1238, 1256	983	743	—	—	—
4	3631	2959–2873	1401 1429 s	1238	1072	885	574	374	281
MBZTH	3112	3077–2838	1497	1320	1013	938	—	—	—
5	3632	2959–2874	1429	1240	1078, 1036	933	571	335	265

Table 2 ^{119}Sn Mössbauer spectroscopic data for complexes **1–5**

Molecule	Temp (K)	δ (mm s^{-1})	D (mm s^{-1})	Area (%)	δ (mm s^{-1})	D (mm s^{-1})	Area (%)	δ (mm s^{-1})	D (mm s^{-1})	Area (%)
1	85	1.38	2.93	100	—	—	—	—	—	—
2	85	1.41	2.39	93	–0.27	0.00	7	—	—	—
3	85	0.14	0.49	72	0.58	2.08	22	1.24	3.30	6
4	85	0.04	0.46	100	—	—	—	—	—	—
5	85	1.24	2.97	48	0.17	0.39	52	—	—	—

Table 3 Characteristic signals in ^1H , ^{13}C NMR spectra of bis-(2,6-di-*tert*-butyl-4-hydroxyphenyl)tin derivatives

Compound	$^1\text{H-NMR}$ δ (ppm)			$^{13}\text{C-NMR}$		$^1J_{\text{C-Sn}}$ (Hz)	Solvent
	$\text{C}(\text{CH}_3)_3$	OH	C_6H_2 ($^3J_{\text{Sn-H}}$, Hz)	δ (ppm)			
1	1.48	5.58	7.51 (84)	30.12, 34.67, 127.48, 131.85, 137.25, 157.00		n.o.	CDCl_3
2	1.38	5.29	7.65 (80)	30.41, 34.62, 115.60, 131.87, 132.13, 135.96, 153.31, 156.68, 175.35		458	CDCl_3
3	1.38	n.o.	7.24 (n.o.)	31.03, 35.02, 35.30, 116.71, 124.95, 133.26, 139.33, 154.50, 157.42, 163.30, 180.59.		401	DMSO-d_6
4	1.44	5.39	7.72 (84)	29.12, 33.53, 117.65, 118.48, 123.17, 123.81, 131.12, 135.08, 137.93, 145.05, 154.72		510	CDCl_3
5	1.39	5.43	7.78 (88)	30.39, 34.40, 111.80, 119.72, 121.62, 124.76, 125.02, 127.30, 131.95, 136.02, 137.37, 153.95, 159.38		503	CDCl_3

n.o. = not observed.

(b) ^{119}Sn Mössbauer spectroscopy. Solid state, ^{119}Sn Mössbauer spectroscopic data at 85 K of complexes **1–5** are given in Table 2 (Fig. S10–S14†).

The spectra of **1**, **2**, **4** and **5** consist of one symmetric Lorentzian doublet, while that of **3** consists of two symmetric Lorentzian doublets. The occurrence of two symmetric Lorentzian doublets indicates the formation of two structural isomers for complex **3**.¹⁴ The values of δ (0.04–1.41 mm s^{-1}) for complexes **1–5** show that tin is at the (4+) oxidation state in all cases.^{6d,14a} Organotin complexes with R_2Sn tetrahedral geometry exhibit quadrupole splitting parameters in the range of 1.70–3.10 mm s^{-1} . Organotin complexes with *trans*- $\text{R}_2\text{Sn}(\text{iv})$ (R = alkyl) and trigonal bipyramidal arrangement around the tin(iv) ion exhibit D values in the range of 2.00–4.00 mm s^{-1} , while those of *cis*- $\text{R}_2\text{Sn}(\text{iv})$ trigonal bipyramidal geometry in the range of 2.17–3.82 mm s^{-1} . *trans*- R_2Sn distorted octahedral

complexes exhibit quadrupole splitting parameters in the region of 2.40–5.50 mm s^{-1} .^{14a} Complex **1** (R_2SnCl_2) with a D value of 2.93 mm s^{-1} is within the tetrahedral complexes, the D value of **2** (2.39 mm s^{-1}) is in agreement for the tin complexes with *trans*- $\text{R}_2\text{Sn}(\text{L}_2)$ octahedral complexes. The quadrupole splitting parameter of **3** is 2.09 mm s^{-1} in the borderline for *cis*- $\text{R}_2\text{Sn}(\text{L}_2)$ trigonal bipyramidal complexes or tetrahedral complexes (see also Raman spectroscopy). The D value of 2.97 mm s^{-1} classified **5** in the *cis*- $\text{R}_2\text{Sn}(\text{L}_2)$ type of complexes. However, the low D value (0.46 mm s^{-1}) in the case of **4** is inconsistent with the *cis*- $\text{R}_2\text{Sn}(\text{iv})$ trigonal bipyramidal geometry found from X-ray diffraction analysis (see Crystal structures).

(c) NMR spectroscopy. ^1H NMR data for complexes **1–5** are given in Table 3 (Fig. S15–S19†). No signals for amide protons were observed in the spectra of thioamide complexes **2–5** in

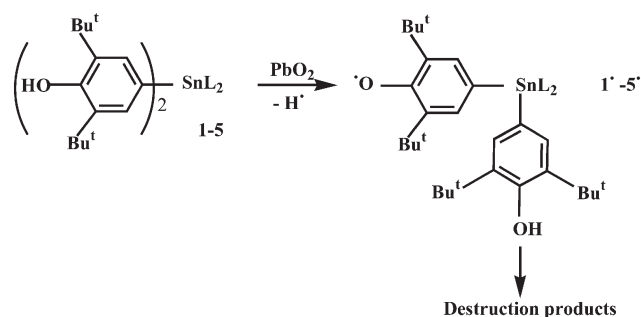
CDCl₃ solution. The characteristic signals of *tert*-butyl protons and hindered phenol groups are shifted to strong field in the spectra of thiol complexes in comparison with those of the chloride one (**1**) confirming the ligand–metal coordination. Furthermore, the aromatic C–H protons show a coupling constant with paramagnetic isotopes ^{117,119}Sn (*S* = 1/2). The *J*(Sn–H) coupling values can be used for the prediction of the structure geometry. The value of ³*J*(Sn–H) in the case of starting bis-aryltin dichloride **1** was found to be equal to 84 Hz that is similar to the one of diorganotin benzoate complex Ph₂SnL₂ (L = 2-[*N*-(2,6-dichloro-3-methylphenyl)amino] benzoate) (76.3 Hz).^{15a} The high value of *J* indicates the strong interaction of the ligand and the acceptors in solution. It was previously demonstrated that the value of ³*J*(Sn–H) for organotin derivatives which possess the same hybridization as that of R₄Sn (e.g. R_nSnX_{4–n}, where *n* = 1–4) could be calculated by using the electronegativity term ($\Delta\chi$) in the relationship

$${}^3J(\text{Sn-H of compound}) = {}^3J(\text{Sn-H of R}_4\text{Sn}) + A\Delta\chi,$$

where *A* is a constant, $\Delta\chi = \Sigma\chi_A - \Sigma\chi_B$; $\Sigma\chi_A$ = sum of electronegativities of the groups attached to the tin in the calculated compound; $\Sigma\chi_B$ = sum of the electronegativities of the groups attached to the metal in the parent compound (R₄Sn). A ³*J* of Ph₄Sn equal to 68 Hz has been previously reported.^{15b}

To deal with the low solubility of **3** in CDCl₃ we used DMSO-*d*₆, the absence of a hydroxyl group signal in the spectrum can be explained by the exchange effect during hydrogen bond formation in this solvent.

The assignment of the ¹³C-NMR spectrum of complex **1** (Fig. S20†) was based on the data of Ph₂SnCl₂^{15c} and those of the organometallic derivatives of 2,6-di-*tert*-butylphenols.^{15d} Complex **1** displays resonance signals at 30.12 (C(CH₃)₃), 34.67 (C(CH₃)₃), 127.48 (C¹ in R), 131.85 (C² in R), 137.25 (C³ in R), 157.00 (C⁴ in R) ppm respectively which are assigned to the CH₃-groups of the *tert*-butyl substituent of phenols and to the carbon atoms of aromatic rings (C¹, C², C³ and C⁴ (Scheme 1)). The most intensive signal is attributed to the aromatic C²–H at 131.85 ppm which has satellites due to Sn–C coupling. The value of ²*J*_{Sn–C} = 80 Hz also points to the tetrahedral geometry of **1** (see also Mössbauer spectroscopy). The signals due to the C² are observed in the spectra of the complexes **2–5** at 132.13 (**2**), 133.26 (**3**), 131.12 (**4**) and 125.02 (**5**) ppm respectively (Table 3, Fig. S21–S24†). The chemical shifts of the carbon atoms of the *tert*-butyl group observed at 30.12, 34.67 ppm in the spectrum of **1** are shifted downfield in the case of bis substitution of Cl atoms by S of PMTH and MPMTH ligands in complexes **2, 3** (30.41, 34.62 ppm (**2**) and 31.03, 35.30 ppm (**3**)), while in the case of the mono substitution of Cl by MPYTH in complex **4**, they are shifted towards strong field (29.12, 33.53 ppm (**4**)). Thus, these shifts in C_(*t*-bu) signals are indicative of the nature of substituents at the Sn atom in the spectra of complexes **2–5**. Moreover, the ¹*J*(¹¹⁹Sn–¹³C) values observed in the ¹³C-NMR spectra of **2–5** are reported in Table 3. The C–Sn–C bond angles of organotin(IV) complexes calculated by the equation ¹*J*(¹¹⁹Sn–¹³C) = 11.4 θ – 875^{7a,15d-f} are 117° (**2**), 112° (**3**), 122° (**4**) and 121° (**5**), respectively, which are in agreement with those found in the solid state by X-ray analysis (127.17(19)° (**2A**), 119.0(2)° (**2B**), 111.44(12)° (**3**), 119.66(12)° (**4A**), 120.23(12)°



Scheme 3

Table 4 Parameters of ESR spectra of phenoxyl radicals (toluene, 293 K)

Compound	<i>g</i> -factor	<i>a</i> (2H) (G)
1	2.0041	1.5
2	2.0041	2.0
3	2.0063	1.5
4	2.0027	^a
5	2.0033	2.0

^a A broad singlet with low intensity was detected.

(**4B**) and 124.79(13)° (**5**) respectively (Table 5)) indicating that these complexes retain their geometry in solution.

(d) EPR spectroscopy. The chemical oxidation of phenol derivatives **1–5** was carried out in toluene using PbO₂ yielding phenoxyl radicals **1'–5'** (Scheme 3).

The X-band EPR spectra measured at 293 K show the spin density distribution in the organic ligands (Fig. S25–S29†). The radicals are stable at room temperature in the absence of dioxygen for several hours. The intensity of radicals derived from diorganotin complexes with mercaptans was lower than that of radical **1'** that may be explained by the influence of electron donor ligands in the distribution of the unpaired electron in the phenoxyl radical. The chloride atoms are electron-acceptor groups and can be involved in radical transformations as well as to increase the stability of radicals. In contrast, the thiol ligands destabilize the corresponding radicals. The EPR spectrum of radical **1'** exhibits multiple signals corresponding to the coupling of the unpaired electron with two non-equivalent groups of *meta*-protons of the phenoxyl ring (1H). The isotropic *g*-values for the radicals **1'–5'** are in the range 2.0041–2.0063 with hyperfine coupling constants derived from protons (Table 4). However, the hyperfine coupling constants with ^{117/119}Sn were not registered due to the low intensity of spectra, moreover the natural content of ¹¹⁷Sn and ¹¹⁹Sn is 7.75 and 8.60%, respectively. Organotin 2,6-di-*tert*-butylphenoxyl radicals generated in the chemical oxidation have been studied earlier.¹⁶ The stability and the values of hyperfine splitting constants of these radicals are influenced by the electron-withdrawing or electron-donating character of the *para*-substituent in the phenyl ring. For instance, the values of *a*(2H) were 1.7 G (*meta*-protons of the phenoxyl ring) and *a*(^{117/119}Sn) were 57.2 and 59.4 G respectively for the radical from bis-methyl-bis(3,5-di-*tert*-butyl-4-hydroxyphenyl)tin.

Table 5 Selected bond lengths (Å) and angles (°) for complexes 1–5 with e.s.d.'s in parentheses

Complex 1	Complex 2 <i>Isomer-A</i>		Complex 2 <i>Isomer-B</i>		Complex 3		Complex 4 <i>Isomer-A</i>		Complex 4 <i>Isomer-B</i>		Complex 5		
(a) Bond lengths (Å)	(a) Bond lengths (Å)		(a) Bond lengths (Å)		(a) Bond lengths (Å)		(a) Bond lengths (Å)		(a) Bond lengths (Å)		(a) Bond lengths (Å)		
Sn–C11	2.3615(14)	Sn1–S2	2.4616(14)	Sn2–S3	2.4631(14)	Sn1–S1	2.4664(8)	Sn1–C11	2.4443(8)	Sn2–C12	2.4467(8)	Sn1–C11	2.4238(9)
Sn–C12	2.3524(16)	Sn1–C9	2.118(5)	Sn2–C23	2.123(5)	Sn1–S2	2.4265(8)	Sn1–S1	2.4504(8)	Sn2–S2	2.4543(8)	Sn1–S1	2.4796(10)
Sn–C1	2.103(6)	S2–C1	1.759(5)	S3–C5	1.760(7)	Sn1–C1	2.115(3)	Sn1–N1	2.412(3)	Sn2–N2	2.392(3)	Sn1–N1	2.483(3)
Sn–C15	2.098(5)	Sn1–N1	2.815	Sn2–N3	2.873	Sn1–C15	2.116(3)	Sn1–C1	2.136(3)	Sn2–C34	2.118(3)	Sn1–C8	2.126(3)
O1–C4	1.373(7)	O1–C12	1.370(7)	O2–C26	1.372(7)	S1–C29	1.767(3)	Sn1–C15	2.136(3)	Sn2–C47	2.138(3)	Sn1–C22	2.117(3)
O2–C18	1.379(7)	O1–H1	0.89(5)	O2–H2A	0.90(5)	S2–C34	1.745(3)	S1–C29	1.756(3)	S2–C65	1.763(4)	S1–C1	1.728(4)
						O1–C4	1.377(4)	O1–C4	1.383(4)	O3–C37	1.378(4)	S2–C1	1.731(4)
						O2–C18	1.374(4)	O2–C18	1.368(5)	O4–C51	1.388(4)	S2–C3	1.741(4)
						O1–H1	0.8199					O1–C11	1.382(4)
						O2–H2A	0.8209					O2–C25	1.383(6)
(b) Angles (°)	(b) Angles (°)		(b) Angles (°)		(b) Angles (°)		(b) Angles (°)		(b) Angles (°)		(b) Angles (°)		
C11–Sn–C12	103.16(5)	S2–Sn1–C9	106.46(14)	S3_b–Sn2–C23	115.01(14)	S1–Sn1–S2	101.57(3)	C11–Sn1–S1	92.63(3)	S2–Sn2–N2	64.67(7)	C11–Sn1–S1	91.19(3)
C11–Sn–C1	103.32(17)	S2–Sn1–S2_a	88.80(5)	C23–Sn2–C23_b	119.0(2)	S1–Sn1–C1	99.24(9)	C11–Sn1–N1	157.16(7)	S2–Sn2–C34	123.23(9)	C11–Sn1–N1	155.32(7)
C11–Sn–C15	103.18(16)	S2–Sn1–C9_a	110.62(15)	S3_b–Sn2–C23_b	107.85(15)	S1–Sn1–C15	109.30(9)	C11–Sn1–C1	97.31(9)	S2–Sn2–C47	113.14(9)	C11–Sn1–C8	99.32(8)
C12–Sn–C1	109.64(19)	S2_a–Sn1–C9	110.62(15)	S3–Sn2–C23_b	115.01(14)	S2–Sn1–C1	113.11(8)	C11–Sn1–C15	98.88(9)	C12–Sn2–S2	93.81(3)	C11–Sn1–C22	98.46(11)
C12–Sn–C15	111.47(16)	C9–Sn1–C9_a	127.17(19)	S3–Sn2–C23	107.85(15)	S2–Sn1–C15	119.56(9)	S1–Sn1–N1	64.61(7)	C12–Sn2–N2	158.43(7)	S1–Sn1–N1	64.15(7)
C1–Sn–C15	123.5(2)	S2_a–Sn1–C9_a	106.46(14)	S3–Sn2–S3_b	88.07(5)	C1–Sn1–C15	111.44(12)	S1–Sn1–C1	117.24(9)	C12–Sn2–C34	96.70(9)	S1–Sn1–C8	115.34(8)
								S1–Sn1–C15	119.53(9)	C12–Sn2–C47	97.88(9)	S1–Sn1–C22	116.05(11)
								N1–Sn1–C1	92.01(11)	N2–Sn2–C34	94.30(11)	N1–Sn1–C8	92.47(10)
								N1–Sn1–C15	94.47(11)	N2–Sn2–C47	92.48(11)	N1–Sn1–C22	92.34(13)
								C1–Sn1–C15	119.66(12)	C34–Sn2–C47	120.23(12)	C8–Sn1–C22	124.79(13)

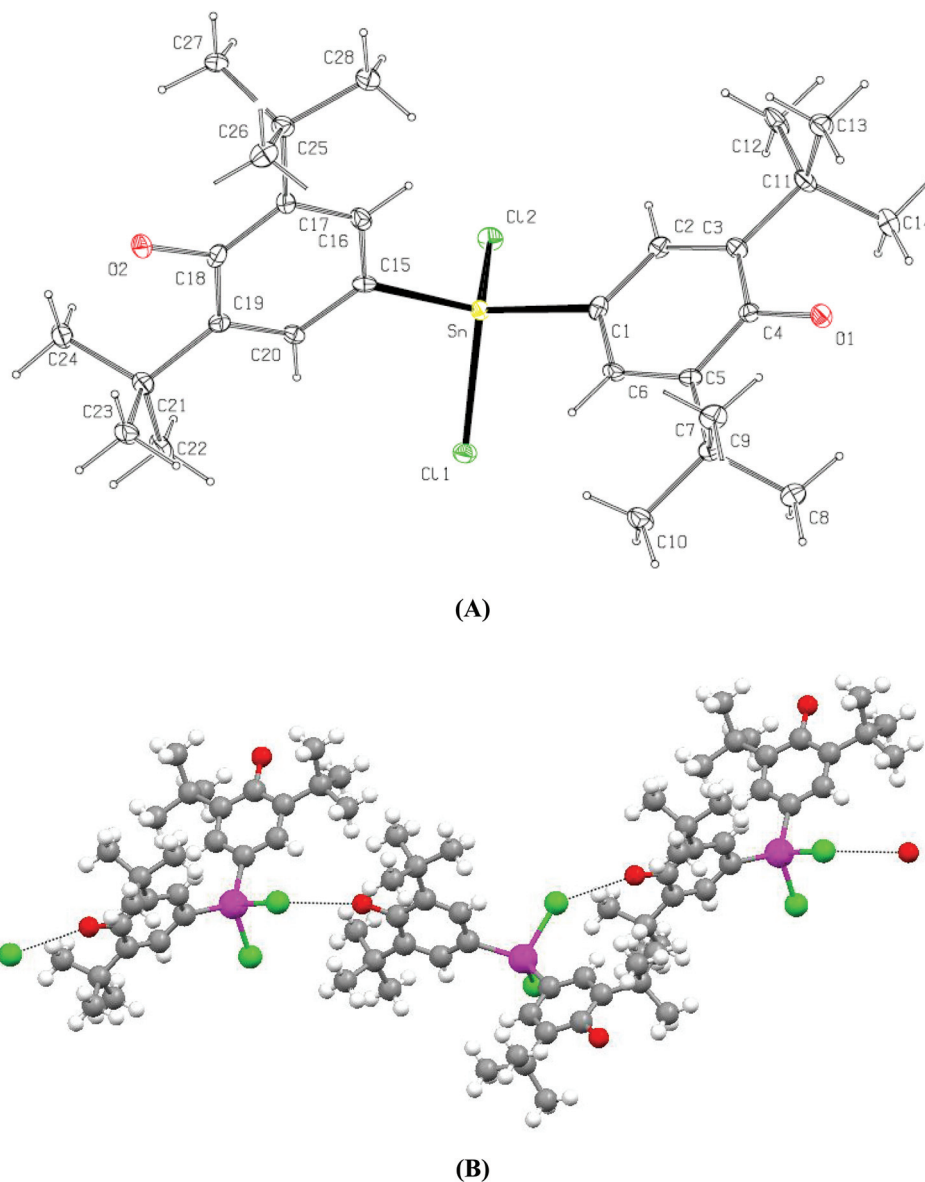


Fig. 1 (A) ORTEP diagram together with the labeling scheme of **1**. (B) Hydrogen bonding interactions lead to a 1D polymeric assembly.

Crystal and molecular structures of $[(\text{tert-Bu})_2(\text{HO-Ph})]_2\text{-SnCl}_2$ (**1**), $\{[(\text{tert-Bu})_2(\text{HO-Ph})]_2\text{Sn(PMT)}_2\}$ (**2**), $\{[(\text{tert-Bu})_2(\text{HO-Ph})]_2\text{Sn(MPMT)}_2\}$ (**3**), $\{[(\text{tert-Bu})_2(\text{HO-Ph})]_2\text{SnCl(PYT)}\}$ (**4**) and $\{[(\text{tert-Bu})_2(\text{HO-Ph})]_2\text{SnCl(MBZT)}\}$ (**5**). ORTEP diagrams of complexes **1–5** are shown in Fig. 1–5, while selected bond distances and angles are given in Table 5.

Compounds **1–5** are covalent monomers in the solid state with distorted tetrahedral (**1**), distorted octahedral (**2**) and distorted trigonal bipyramidal (**3**, **4** and **5**) geometries around the metal centers. In the case of complexes **2** and **4** two isomers were isolated in their unit cells (Fig. 2 and 4).

In the case of complex **1**, the bond angles around tin(IV) varied between $103.16(5)$ and $123.5(2)^\circ$ (Table 5) with the smaller one corresponding to the Cl–Sn–Cl and the longer to the C–Sn–C bond angle respectively due to the valence shell electron pair repulsions. The Sn–Cl bond distances (Sn–Cl1 = $2.3615(14)$ and Sn–Cl2 = $2.3524(16)$ Å respectively) are shorter

than the corresponding bond distances found in complexes **4** and **5** (Sn1–Cl1 = $2.4443(8)$ Å (**4-isomer A**), Sn2–Cl2 = $2.4467(8)$ Å (**4-isomer B**) and Sn1–Cl1 = $2.4238(9)$ Å (**5**)) and in $[(\text{C}_6\text{H}_5)_2\text{SnCl(HMNA)}]$ (H_2MNA = 2-mercapto-nicotinic acid) (Sn(1A)–Cl(1A) = $2.4246(19)$, Sn(1B)–Cl(1B) = $2.424(2)$ Å),^{6a} where one chlorine atom has been replaced by the S,N-thionate anion which chelates the metal ion. This is attributed to the variation in the coordination modes between complex **1** (four coordinated Sn(IV) ion) and **4** or **5** (five coordinated Sn(IV) ion) which leads to different geometries (tetrahedral (**1**) and trigonal bipyramidal (**4**, **5**)).

Intra-molecular interactions Cl11...O1_c = $3.103(4)$ Å [symmetry operation $c = x, 1/2 - y, 1/2 + z$] lead to a supra-molecular assembly of **1** (Fig. 1B).

In the case of **2** two *trans*-aryl groups are bonded to the tin atom (Sn1–C9 = $2.118(5)$ Å (**2-isomer A**) and Sn2–C23 = $2.123(5)$ Å (**2-isomer B**)) forming the axis of the octahedron.

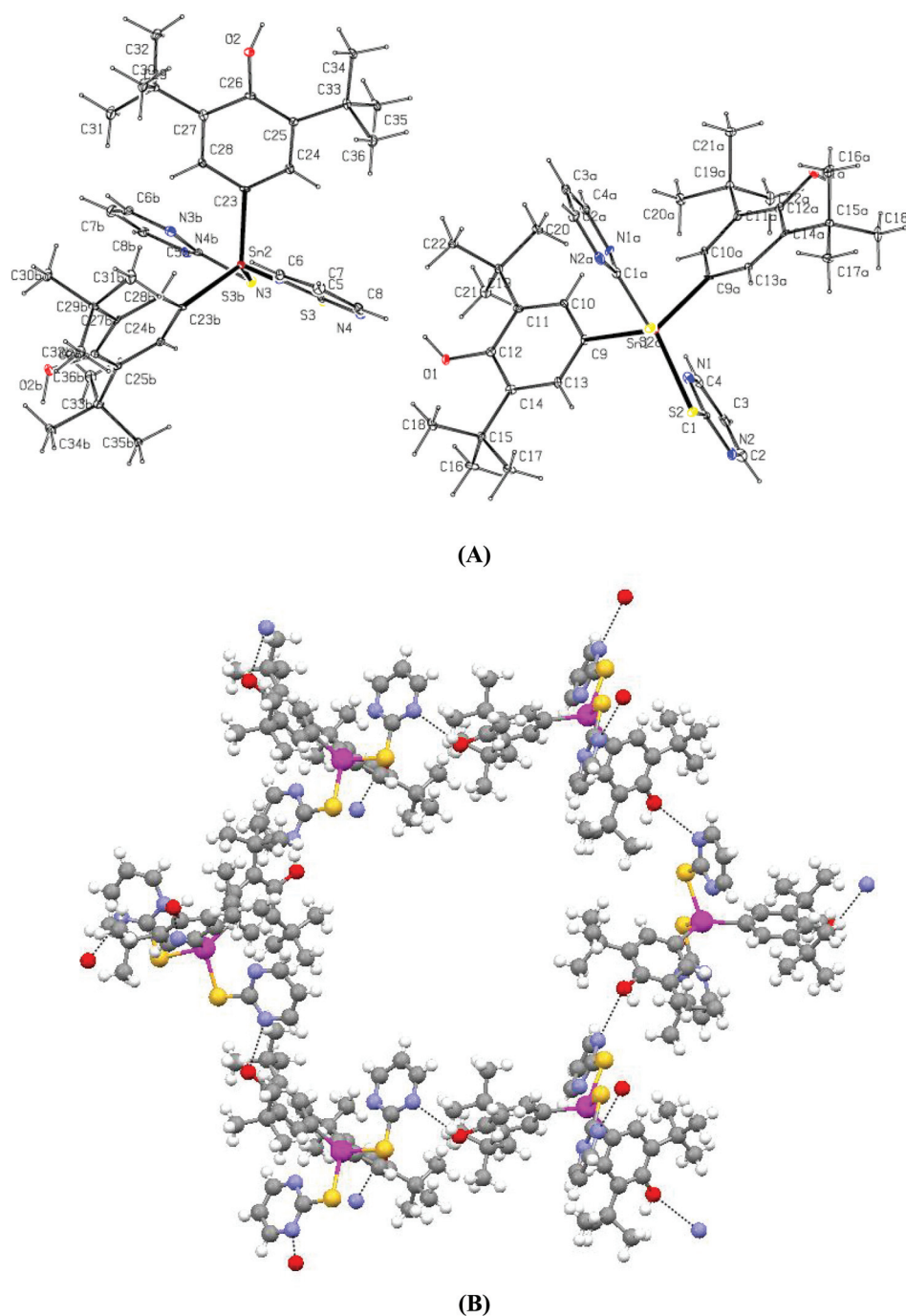


Fig. 2 (A) ORTEP diagram together with the labeling scheme of **2**. (B) Hydrogen bonding interactions lead to a polymeric assembly which turns out to be a ring.

Two deprotonated PMTH ligands are also bonded to the tin atom *via* sulfur (Sn1–S2 = 2.4616(14) Å, Sn2–S3 = 2.4631(14) Å for **2A** and **2B** respectively). The Sn–S bond lengths are in accordance with those previously reported for diorganotin complexes with octahedral geometries as in the complexes [(C₆H₅)₂Sn(cmbzt)₂] (Hcmbzt = 5-chloro-2-mercaptobenzothiazole) where Sn1–S12 = 2.4947(7), Sn1–S22 = 2.5020(7) Å (isomer A) and Sn1–S12 = 2.4947(7), Sn1–S22 = 2.5020(7) Å (isomer B)^{6d} and in [(*n*-C₄H₉)₂Sn(cmbzt)₂] where Sn1–S12 = 2.5042(19), Sn1–S22 = 2.5286(19) Å.^{6d} Moreover, the Sn–S bond distances

found in **2** are in the range to those found for complexes with trigonal bipyramidal geometry (Sn1–S2 = 2.4265(8) Å (**3**), Sn1–S1 = 2.4504(8) Å (**4A**), Sn2–S2 = 2.4543(8) Å (**4B**) and Sn1–S1 = 2.4796(10) Å (**5**)). Triorganotin complexes of thioamides with trigonal bipyramidal geometry also exhibit similar Sn–S bond distances (Sn1A–S2A = 2.4540(15) Å (isomer A) and Sn1A–S2A = 2.4540(15) Å (isomer B) in [(C₆H₅)₃Sn(mbzt)] (Hmbzt = 2-mercaptobenzothiazole),^{6d} Sn1–S12 = 2.4699(9) Å in [(C₆H₅)₃Sn(mbzo)] (Hmbzo = 2-mercaptobenzoxazole)^{6d} and Sn1–S1 = 2.458(3) Å (isomer A) and Sn2–S3 = 2.456(3) Å

(isomer B) in $[(C_6H_5)_3Sn(cmbzt)]$ (Hcmbzt = 5-chloro-2-mercaptobenzothiazole).^{6d}

The octahedral geometry is completed by two weak Sn–N interactions between the nitrogen atoms of the ligands and the

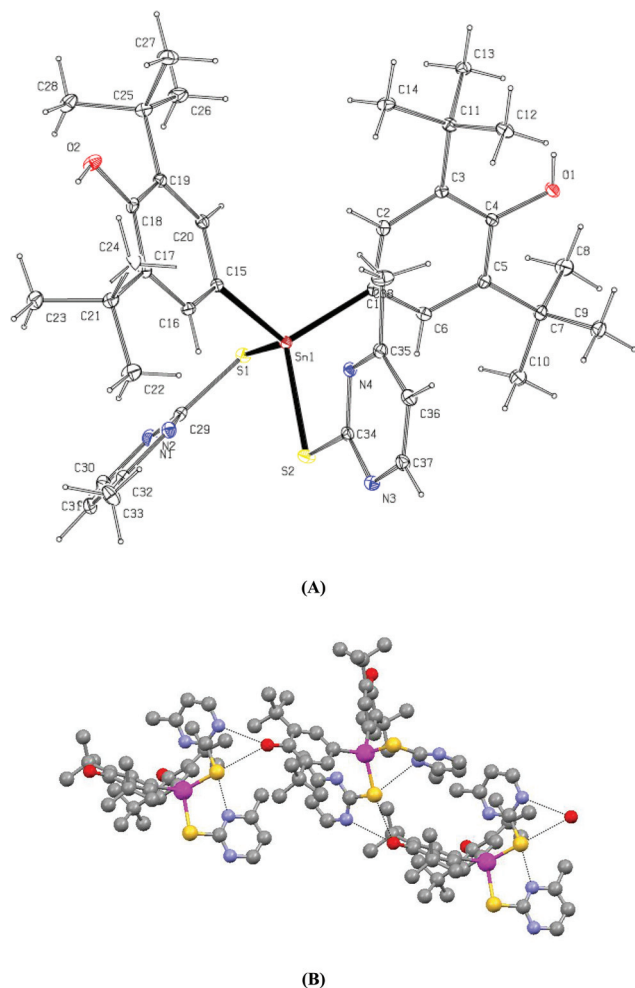


Fig. 3 (A) ORTEP diagram together with the labeling scheme of **3**. (B) Hydrogen bonding interactions lead to a 1D polymeric assembly.

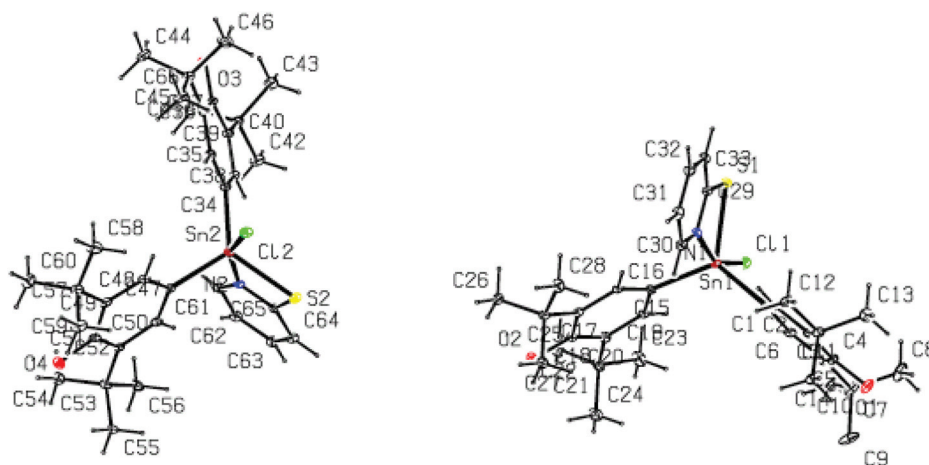


Fig. 4 ORTEP diagram together with the labeling scheme of **4**.

metal center (Sn1–N1 = 2.815 Å (**2A**) and Sn2–N3 = 2.873 Å (**2B**)). These bond distances are in accordance with the corresponding bond lengths found in other complexes with octahedral geometry as in $[(C_6H_5)_2Sn(cmbzt)_2]$ (Hcmbzt = 5-chloro-2-mercaptobenzothiazole) with Sn1–N13 = 2.653(2), Sn1–N23 = 2.7718(18) Å (isomer A) and Sn1–N13 = 2.653(2), Sn1–N23 = 2.7718(18) Å (isomer B)^{6d} and in $[(n-C_4H_9)_2Sn(cmbzt)_2]$ where Sn1–N13 = 2.748(7), Sn1–N23 = 2.766(7) Å.^{6d} However, the Sn–N bond distances in **2** are significantly longer than those found in complexes with trigonal bipyramidal geometries which retain the chlorine atoms as in **4**: Sn1–N1 = 2.412(3), Sn2–N2 = 2.392(3) Å and **5**: Sn1–N1 = 2.483(3) Å. Furthermore, the Sn–N bond lengths become significantly longer in complexes of trigonal bipyramidal geometry without chlorine atoms as in $[(C_6H_5)_3Sn(mbzt)]$ (Hmbzt = 2-mercaptobenzothiazole) (Sn1A–N3A = 2.945(4) Å (isomer A) and (Sn1B–N3B = 2.898(4) Å (isomer B)),^{6d} in $[(C_6H_5)_3Sn(mbzo)]$ (Hmbzo = 2-mercaptobenzoxazole) (Sn1–N11 = 3.067(3) Å)^{6d} and in $[(C_6H_5)_3Sn(cmbzt)]$ (Hcmbzt = 5-chloro-2-mercaptobenzothiazole) (Sn1–N8 = 3.007(4) Å (isomer A) and Sn1–N34 = 3.010(3) Å (isomer B)).^{6d}

The C–S–Sn–S torsion angles found in **2** (S2′–Sn1–S2–C1 = 173.3° for **2A** and S3′–Sn2–S2–C5 = 173.9° for **2B** respectively) indicate the almost co-planar arrangement of the N, C, Sn and S atoms. Thus, the conformation around the tin atom is *trans-C*₂, *cis-N*₂, *cis-S*₂. The C–Sn–C bond angles of **2** (C9–Sn1–C9_a = 127.17(19)° (**2A**), C23–Sn2–C23_b = 119.0(2)° (**2B**)) are shorter than those previously found in $[(C_6H_5)_2Sn(cmbzt)_2]$ (Hcmbzt = 5-chloro-2-mercaptobenzothiazole) with C41–Sn1–C31A = 137.7(5)° (isomer A) and C41–Sn1–C31B = 129.8(7)° (isomer B)^{6d} and in $[(n-C_4H_9)_2Sn(cmbzt)_2]$ where C31–Sn1–C41 is 131.8(3)°.^{6d}

The supra-molecular assembly of **2** (Fig. 2B) is constructed by strong hydrogen bonds O1[H1]⋯N4 = 2.931(6) Å.

In the case of complex **3** the trigonal bipyramidal geometry is established by two carbon atoms from the aryl groups and one sulfur (S2) atom from the MPMTM ligand which form the basal triangle and one S1 and one N4 atom from the two MPMTM ligands form the axis. Two de-protonated MPMTM ligands are bonded to the tin atom (Sn1–S1 = 2.4664(8) and Sn1–S2 =

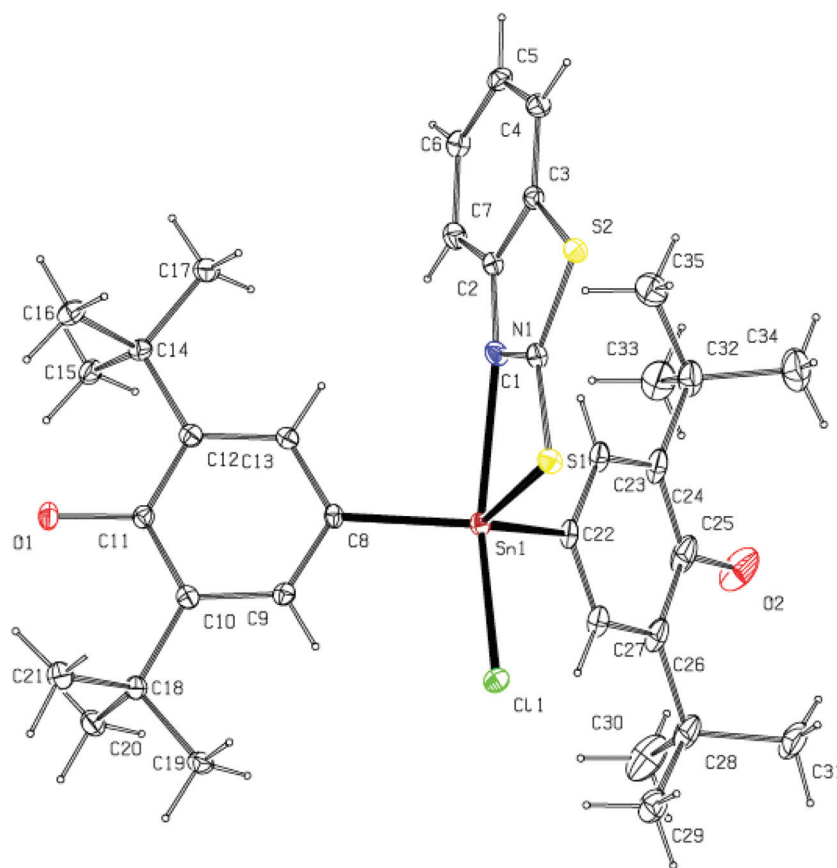


Fig. 5 ORTEP diagram together with the labeling scheme of **5**.

2.4265(8) Å). The Sn–C bonds are Sn1–C1 = 2.115(3) and Sn1–C15 = 2.116(3) Å. It is noteworthy to mention that only one of the two MPMTM ligands interacts with the tin(IV) ion through Sn–N (Sn1–N4 = 2.763 Å) bonding interaction, while the corresponding Sn1–N2 distance of the second MPMTM is 3.028 Å. To ensure the trigonal bipyramidal geometry adopted by **3**, the geometric parameter τ^{17a} ($\tau = (\alpha - \beta)/60$ where α is the greatest and β the second greatest bond angle around the metal center) is determined.^{17a} The τ value is equal to zero for perfectly tetragonal pyramidal geometry and unity for perfectly trigonal bipyramidal geometry. The calculated value for **3** is 0.68, indicating distorted trigonal bipyramidal geometry.

Strong hydrogen bonds are also formed O1[H1]...N3 = 2.993(3) Å (Fig. 3B). The strong hydrogen bonding interaction which may prohibit the free rotation of phenol groups together with the variation in the coordination mode of the MPMTM ligands towards Sn(IV) might be affected in the environment of the H[C2] atoms of the phenyl rings resulting in the two signals observed in the H-NMR spectrum of **3** (see Experimental part).

The structures of compounds **4**, **5** consist of [Ar₂Sn(IV)] moieties. The stereochemistry around the Sn(1) atom is trigonal bipyramidal, with the equatorial plane being defined by N1, S1 and C11 atoms (**4A**) and N2, S2 and Cl2 atoms (**4B**). Thus, a unique structure with an axial–equatorial arrangement of the phenyl groups at Sn(1) is formed. These complexes (**4**, **5**) are examples of a pentacoordinated Ph₃SnXY system with an axial–equatorial arrangement of the phenyl groups at the Sn(1) center.

The calculated τ values^{17a} are 0.63 (**4A**), 0.59 (**4B**) and 0.51 (**5**) respectively.

The C–O bond distances found in complexes **1–5** lie between 1.368(5) (**4A**) to 1.388(4) (**4B**) Å which are shorter than the av. value of 1.43 Å of alcoholic C–O[H] and longer than the av. value of 1.24 Å of the C=O bond,^{17b} indicating partial double bonding interaction. This might be due to the deprotonation of these oxygen atoms with the simultaneous formation of the radical (Scheme 3).

Biological tests. The cytotoxicity of the complexes **1–5** against human breast adenocarcinoma (MCF-7) has been evaluated by means of the Trypan blue method. The IC₅₀ (μM) values are 3.12 ± 0.38 (**1**), 7.86 ± 0.87 (**2**), 0.58 ± 0.10 (**3**), >30 (**4**) and >30 (**5**) μM (Table 6). The corresponding IC₅₀ value of cisplatin is 18.5 μM.^{7a} Thus complexes **1–3** exhibit stronger activity than cisplatin against MCF-7. Among **1–5**, the strongest activity was found for **3** (with trigonal bipyramidal geometry), which is 32-fold stronger than that of cisplatin. It is mentioned that complexes **4** and **5** show almost negligible activity although they both have trigonal bipyramidal geometry. These two complexes retain the chlorine atoms on the tin(IV) cation, while they both exhibit strong metal–ligand linkage (Sn–N bond 2.412(3) (**4A**), 2.392(3) (**4B**) and 2.483(3) (**5**) Å, see Crystal structures).

Table 6 summarizes the IC₅₀ values for cell viability found for organotin(IV)–thioamide compounds against MCF-7 (human breast adenocarcinoma), HeLa (human cervix carcinoma), WiDr

Table 6 IC₅₀ values for cell viability found for compounds 1–5 and other organotin(IV)-thioamide complexes against MCF-7 (human breast adenocarcinoma), HeLa (human cervix carcinoma), WiDr (human colon carcinoma), OAW-42 (ovarian), A549 (lung), MDA-MB-231 (breast, ER negative), Caki-1 (renal), LMS (leiomyosarcoma) cell lines

Compounds	IC ₅₀ (μM)								Geometry	Ref.
	MCF-7	HeLa	WiDr	OAW-42	A-549	MDA-MB-231	Caki-1	LMS		
1	3.12 ± 0.38								Tetrahedral	*
2	7.86 ± 0.87								Disorder octahedral	*
3	0.58 ± 0.1								Trigonal bipyramidal	*
4	>30								Trigonal bipyramidal	*
5	>30								Trigonal bipyramidal	*
Cisplatin	18.5							6.53 ± 0.43	Square planar	7a,18
{[Ph ₃ Sn(O-HTBA)·0.7H ₂ O]} _n ^a	0.103	0.105	0.2	0.235	0.203	0.12	0.133		Trigonal bipyramidal	7a
[(n-Bu) ₃ Sn(O-HTBA)·H ₂ O] ^a	0.068	0.065	0.072	0.24	0.106	0.406	0.125		Trigonal bipyramidal	7b
{[Ph ₃ Sn] ₂ (MNA)·[(CH ₃) ₂ CO]} ^b	0.0299							0.02	Trigonal bipyramidal	19
[(n-Bu) ₂ Sn(2-pyridinethiolato- <i>N</i> -oxide) ₂]	0.1154		0.43						Skew-trapezoidal bipyramid	19a
[Ph ₂ Sn(2-pyridinethiolato- <i>N</i> -oxide) ₂]	0.5636		2.26						Distorted <i>cis</i> octahedral	19a
[(Ph-CH ₂) ₂ Sn(2-pyridinethiolato- <i>N</i> -oxide) ₂]	0.5404		1.68						Distorted <i>cis</i> octahedral	19a
[Ph ₃ Sn(PMTH)] ^c								0.1	Trigonal bipyramidal	19b
[(n-Bu) ₂ Sn(PMTH) ₂] ^c								0.65	Disorder octahedral	19b
[Ph ₂ Sn(PMTH) ₂] ^c								1.0–2.0	Disorder octahedral	19b
[Me ₂ Sn(PMTH) ₂] ^c								20–60	Disorder octahedral	19b
[Ph ₃ Sn(MBZO)] ^d								1.3–3	Trigonal bipyramidal	19c
[Ph ₃ Sn(MBZT)] ^e								1.5–3	Trigonal bipyramidal	19c
[Ph ₃ Sn(CMBZT)] ^f								0.5–0.8	Trigonal bipyramidal	19c
[(n-Bu) ₂ Sn(MBZT) ₂] ^e								2.5	Distorted octahedral	19c
[Me ₂ Sn(CMBZT) ₂ ·1.7(H ₂ O)] ^f								5–7.5	Distorted octahedral	19c
[Bu ₂ Sn(CMBZT) ₂] ^f								0.6–0.8	Distorted octahedral	19c
[Ph ₂ Sn(CMBZT) ₂] ^f								0.3–0.5	Distorted octahedral	19c

*This work. ^aH₂TBA = 2-thiobarbituric acid. ^bH₂MNA = 2-mercapto-nicotinic acid. ^cPMTH = 2-mercapto-pyrimidine. ^dMBZOH = 2-mercapto-benzoxazole. ^eMBZTH = 2-mercapto-benzothiazole. ^fCMBZTH = 5-chloro-2-mercapto-benzothiazole.

(human colon carcinoma), OAW-42 (ovarian), A549 (lung), MDA-MB-231 (breast, ER negative), Caki-1 (renal), LMS (leiomyosarcoma) cancer cell lines. It is shown that diorganotin(IV) complexes with disorder octahedral geometry exhibit less activity than those of triorganotin(IV) with trigonal bipyramidal geometry. Also the complexes {[Ph₃Sn(O-HTBA)·0.7H₂O]}_n and [(n-Bu)₃Sn(O-HTBA)·H₂O] show selective cytotoxic activity against carcinoma cells, especially against HeLa (human cervical carcinoma) and MCF-7 (human breast adenocarcinoma) cells, than against sarcoma (leiomyosarcoma cells) or other cell lines of carcinoma.^{7a} This strong selective activity of [(n-Bu)₃Sn(O-HTBA)·H₂O] and {[Ph₃Sn(O-HTBA)·0.7H₂O]}_n⁷ complexes against MCF-7 (ER positive) is not observed when they

were tested against breast cancer cells (MDA-MB-231) (breast, ER negative), indicating that estrogen receptors (ER) may be also involved in their antitumor mechanism.^{7a} The high cytotoxic activity of complex **3** against MCF-7 cells might also be attributed to the stable radical detected (see EPR studies) and its blocking capacity of estrogen receptors as observed in the case of [(n-Bu)₃Sn(O-HTBA)·H₂O] and [Ph₃Sn(O-HTBA)·0.7H₂O] complexes.

Apart from thioamides, polyoxaalkyltin complexes of carboxylic acids were also tested for their antitumor activity.^{3b} Thus, complexes with formulae (n-Bu)₈Sn₄O₂(L1)₄ (MW = 1496.24 g mol⁻¹) (n-Bu)₈Sn₄O₂(L2)₄ (MW = 1672.45 g mol⁻¹), Ph₃Sn(L3) (MW = 661.33 g mol⁻¹), and (n-Bu)₃Sn(L3) (MW =

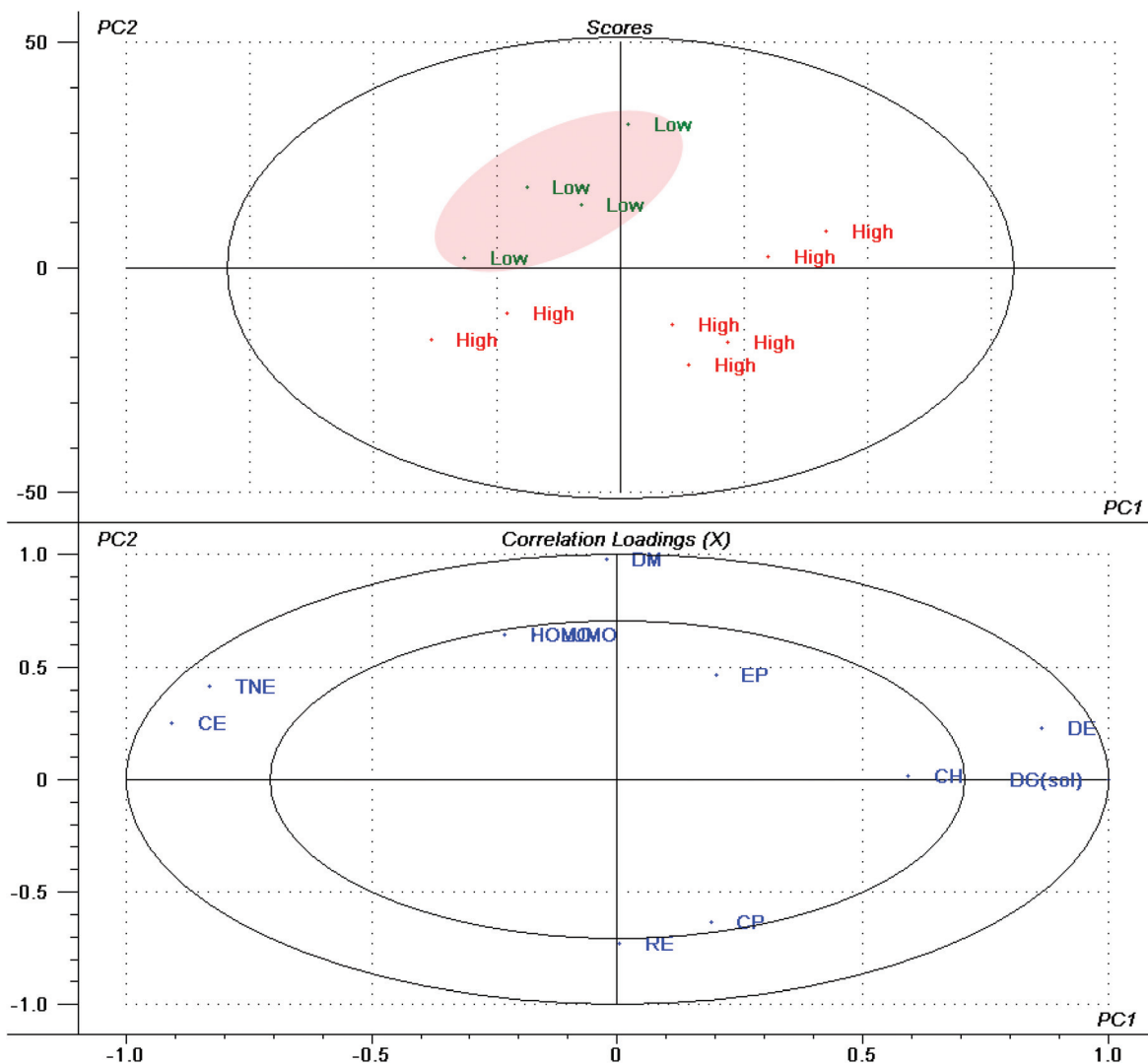


Fig. 6 PCA scores and correlation loadings plot for PC1 and PC2. A clustering pattern is achieved for samples with $IC_{50} > 1$ (low) and $IC_{50} < 1$ (high).

601.36 g mol⁻¹) (where HL1 = CH₃O(CH₂CH₂O)CH₂COOH or C₅H₉O₄, HL2 = CH₃O(CH₂CH₂O)₂CH₂COOH or C₇H₁₃O₃ and HL3 = benzocrownCOOH or C₁₅H₁₃O₃) have been tested against human tumor cell lines, MCF-7, EVSA-T (breast cancer cells), WiDr (a colon cancer), IGROV (an ovarian cancer), M19 MEL (a melanoma), A498 (a renal cancer) and H226 (a lung cancer). Among them, complex (*n*-Bu)₈Sn₄O₂(L2)₄ exhibits the strongest activity against cancer cell lines with IC_{50} values less than 0.0006 μM (or 1 ng ml⁻¹) against MCF-7, EVSA-T, IGROV, M19 MEL, A498 and H226 cell lines respectively, while against WiDr its IC_{50} value is less than 0.0026 μM (or <1.8 ng ml⁻¹).^{3b} These IC_{50} values indicate far higher cytotoxic activity of this type of organotin complex than that of **1–5**. However, in contrast to the organotin complexes of thioamides with formulae [(*n*-Bu)₃Sn(O-HTBA)·H₂O] and [Ph₃Sn(O-HTBA)·0.7H₂O], the complexes of benzocrown carboxylic acid HL3 (Ph₃Sn(L3) and (*n*-Bu)₃Sn(L3)) show higher activity against the ER-negative cell line (EVSA-T) (the IC_{50} value is <0.003 μM or <2 ng ml⁻¹ for both complexes) than against the MCF-7 cell line (ER-positive cell line) (where the IC_{50} values

are 0.0044 μM or 2.9 ng ml⁻¹ and 0.0055 μM or 3.3 ng ml⁻¹ respectively).^{3b} Since both types of organotin(IV) complexes with either the thioamide (H₂TBA) or the benzocrown carboxylic acid (HL3) adopt similar geometry (trigonal bipyramidal), the alteration in biological activity might be due to the different kinds of ligands (thioamides or polyoxa-carboxylic acids) used.

Computational studies – multivariate statistical analysis. In an effort to quantify the inhibition activity against MCF-7 of similar organotin complexes (included in Table 6), as this is expressed by the corresponding IC_{50} values, we used a combination of a descriptive analysis based on density functional theory (DFT) methods and principal components analysis (PCA) algorithms. The first two PCs are depicted in Fig. 6 explaining almost the total variance of the data. The plot shows distinct group clustering especially for the cases with low inhibitory action ($IC_{50} > 1$) indicating that IC_{50} is a significant discriminating factor effectively explained by the physicochemical characteristics under study. The Hotelling T² ellipse, indicating the

95% confidence limit, reveals no potential outliers lying outside the ellipse. By inspecting the correlation loadings plot, we conclude that significant properties for the complexes with limited inhibition activity ($IC_{50} > 1$) are DM, CE and TNE while for complexes with $IC_{50} < 1$ the most statistically significant properties are DG(sol) and DE which are negatively correlated with CE and TNE. Far less significant, in this case, is DM. Thus, DM is inversely correlated with biological activity and decreasing the polarity of a molecule belonging to a related organotin set of complexes will increase its biological effectiveness.

To relate the variation of the IC_{50} values (dependent variable) to the variations of energetic parameters (independent variables) calculated from DFT studies and statistically indexed by PCA, we have carried out partial least squares (PLS) regression analysis. This method performs particularly well when the X-data are correlated like in this case (energy related terms). In the calculations we have included the descriptors which were shown as highly significant by the PCA, namely DM, CE and TNE for the complexes with low activity and DG(sol), CE, TNE, RE and DM for the complexes with high activity. In constructing the latent components in PLS from the available set of descriptors we have found that the most relevant descriptors are DM and DG(sol) as expected from the initial PCA analysis. The models developed by PLS regression analysis are given by the following expressions:

$$IC_{50} (\text{low}) = -0.079 * CE - 1.77 * TNE - 1.29 * DM + 154.06$$

and

$$IC_{50} (\text{high}) = -0.002 * DG(\text{sol}) - 0.013 * CE + 0.110 * DE - 0.005 * TNE + 0.030 * DM - 0.62.$$

Fig. 7 depicts the graphical representations of the above linear equations and the fitting parameters ($r^2 = 0.93$ for both cases).

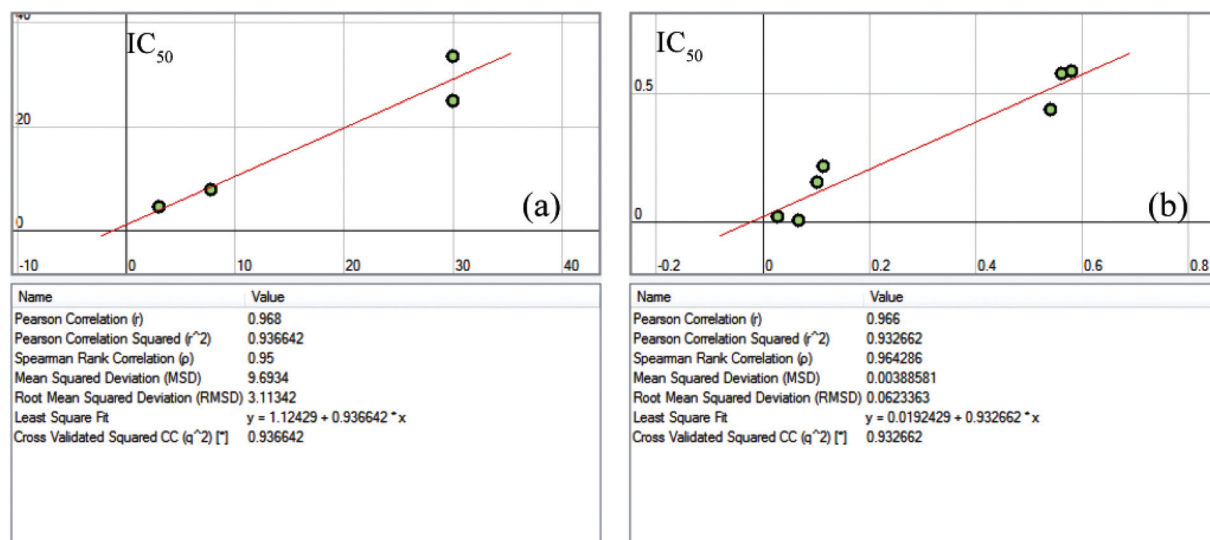


Fig. 7 PLS regression analysis for organotin complexes with low (a) and high (b) biological activity.

Conclusions

Aiming at the development of new antitumor agents, the antioxidant 2,6-di-*tert*-butylphenol fragments and different S-donor ligands were combined with tin(IV) cations. Thus, five diorganotin(IV) complexes with the 2,6-di-*tert*-butylphenol moiety with various thioamides were synthesized and structurally characterized. The geometries adopted varied from the tetrahedron dichloride $[(\text{tert-Bu})_2(\text{HO-Ph})_2\text{SnCl}_2]$ (**1**), distorted octahedral in $\{[(\text{tert-Bu})_2(\text{HO-Ph})_2\text{Sn}(\text{PMT})_2]\}$ (**2**) and trigonal bipyramidal in $\{[(\text{tert-Bu})_2(\text{HO-Ph})_2\text{Sn}(\text{MPMT})_2]\}$ (**3**), $\{[(\text{tert-Bu})_2(\text{HO-Ph})_2\text{SnCl}(\text{PYT})]\}$ (**4**) and $\{[(\text{tert-Bu})_2(\text{HO-Ph})_2\text{SnCl}(\text{MBZT})]\}$ (**5**). The cytotoxicity of **1–5** against MCF-7 has been also evaluated. Complex **3** shows strong such activity ($IC_{50} = 0.58 \pm 0.1 \mu\text{M}$).

According to Huber *et al.*²⁰ the structures of all active compounds are characterized by (i) the availability of coordination positions at Sn and (ii) the occurrence of relatively stable ligand–Sn bonds, *e.g.* Sn–N and Sn–S, and their slow hydrolytic decomposition. In agreement with that, the significant strong anti-cancer activity evaluated for **3** is attributed to the availability of coordination positions around Sn(IV) ions of the five coordinated tin(IV) atom. The negligible anti-tumor activity shown by compounds **4** and **5**, on the other hand, can be ascribed to their high stability as a result of the very strong ligand–tin(IV) coordination bonding interactions (Sn–S, Sn–N bonds), which might be due to the presence of chlorine atoms on the tin ion.

Organotin(IV) complexes of thioamides show selective activity against human breast adenocarcinoma (MCF-7) cells (Table 6). This strong selective activity in the case of $[(n\text{-Bu})_3\text{Sn}(\text{O-HTBA}) \cdot \text{H}_2\text{O}]$ and $\{[\text{Ph}_3\text{Sn}(\text{O-HTBA}) \cdot 0.7\text{H}_2\text{O}]_n\}$ complexes was observed against MCF-7 (ER positive) but not against breast cancer cells (MDA-MB-231) (breast, ER negative). This indicates that estrogen receptors (ER) may be involved in their antitumor mechanism.^{7a} Complexes of benzocrown carboxylic acid $\text{Ph}_3\text{Sn}(\text{L3})$ and $(n\text{-Bu})_3\text{Sn}(\text{L3})$,^{3b} on the other hand, adopt trigonal bipyramidal geometry, however they show higher activity against the ER-negative cell line (EVSA-T)

than against the MCF-7 cell line (ER-positive cell line),^{3b} indicating that this alteration might be due to the different kinds of ligands (thioamides or polyoxa-carboxylic acids) used.

The high cytotoxic activity of complex **3** against MCF-7 cells might also be attributed to the stable radical detected (see EPR studies) and its blocking capacity of estrogen receptors.

4. Experimental

Materials and instruments

All solvents used were of reagent grade, while thioamides (Aldrich, Merck) were used with no further purification. 2-Mercapto-4-methyl-pyrimidine was used in the form of hydrochloride MPMT·HCl (Aldrich, 99%). Di-(3,5-di-*tert*-butyl-4-hydroxyphenyl)titan dichloride was prepared as described previously.¹² Infrared spectra in the region of 4000–370 cm⁻¹ were obtained in KBr pellets. The ¹H, ¹³C-NMR spectra were recorded on a Bruker AC 250, 400 MHFT-NMR instrument in CDCl₃ or DMSO-d₆. Chemical shifts are given in ppm using ¹H-TMS as an internal reference. Elemental analysis for C, H, N and S was carried out with a Carlo Erba EA MODEL 1108. The samples were dissolved in CHCl₃ and put at target. The ¹¹⁹Sn Mössbauer spectra were collected at various sample temperatures (85–150 K) with a constant acceleration spectrometer equipped with a CaSnO₃ source kept at low temperature. ESR spectra were recorded on the Bruker EMX spectrometer at X-band frequency (9.8 GHz). The measurements were carried out after pre-evacuation (10⁻² Torr) of tubes with solutions in toluene of samples (concentration 1 × 10⁻⁴ mol L⁻¹). The oxidant PbO₂ (Aldrich) was taken in a tenfold excess.

Synthesis of complexes 2–5

Complexes **2–5** were prepared as follows. 0.4 mmol of the appropriate thiol ligand (45 mg PMTH, 50 mg MPMT, 45 mg PYTH, 65 mg MBZTH) was suspended in 5 ml H₂O and 0.4 ml 1 M KOH (0.4 mmol) was then added. The mixture was stirred until clearness. In the case of MPMT·HCl 2 equiv. of KOH were added. A solution of 120 mg of **1** (0.2 mmol) in 3 ml MeOH was then added to the previous solution. A white precipitate formed immediately, while the mixture was stirred for 1 h. The precipitate was filtered off, washed with 5 ml of cold distilled water and dried in air overnight.

Crystals of **1** were obtained by slow evaporation of an *o*-xylene solution. Colorless crystals of **2** and **4** suitable for X-ray analysis were formed by slow evaporation of a methanol–acetonitrile solution (1 : 1), while crystals of **3** and **5** were obtained by slow diffusion of hexane in CHCl₃ solutions.

1; R₂SnCl₂: Mol. Wt.: 600.24; m.p. 234–235 °C. IR (cm⁻¹): 3614 s, 2963 s, 2872 m, 1571 m, 1480 m, 1446 m, 1427 s, 1317 s, 1241 s, 1143 s, 1120 s, 930 w, 874 m, 808 w, 776 m, 606 w, 568 m, 376 s. ¹H-NMR (δ (ppm), CDCl₃): 1.49 (s, 36 H, C(CH₃)₃); 5.58 (s, 2 H, OH); 7.52 (s, ³J_{H-Sn} = 82 and 86 Hz, 4 H, C²H in R). ¹³C-NMR (δ (ppm), CDCl₃): 30.12 (C(CH₃)₃), 34.67 (C(CH₃)₃), 127.48 (C¹ in R), 131.85 (²J_{C-Sn} = 76 Hz, C² in R), 137.25 (C³ in R), 157.00 (C⁴ in R).

2; R₂Sn(PMT)₂: Mol. Wt.: 751.63; Yield 71%; m. p. 189–191 °C. Elemental analysis, found: C: 57.39; H: 6.66;

N: 7.18; S: 8.52%, calculated for C₃₆H₄₈N₄O₂S₂Sn: C: 57.53; H: 6.44; N: 7.45; S: 8.53%. IR (cm⁻¹): 3648 w, 3420 broad, 2967 s, 2872 m, 1715 m, 1565 m, 1543 m, 1427 m, 1377 s, 1220 w, 1181 m, 1121 w, 989 w, 872 w, 803 w, 773 w, 748 w, 640 w, 575 w, 375 s. ¹H-NMR (δ (ppm), CDCl₃): 1.38 (s, 36 H, C(CH₃)₃); 5.29 (s, 2 H, OH); 6.89 (t, 2 H, ³J_{HH} = 5 Hz, C⁵H in PMT); 7.65 (s, ³J_{H-Sn} = 80 and 83 Hz, 4H, C²H in R); 8.33 (d, 4 H, ³J_{HH} = 5 Hz, C⁴H in PMT). ¹³C-NMR (δ (ppm), CDCl₃): 30.41 (C(CH₃)₃), 34.62 (C(CH₃)₃), 115.60 (C⁵ in PMT), 131.87 (C³ in R), 132.13 (²J_{C-Sn} = 68 Hz, C² in R), 135.96 (¹J_{C-Sn} = 458 Hz, C¹ in R), 155.31 (C⁴ in R), 156.68 (C^{4,6} in PMT), 175.35 (C² in PMT). ¹¹⁹Sn-NMR (δ (ppm), CDCl₃): -406.87 (Fig. S30†).

3; R₂Sn(MPMT)₂: Mol. Wt.: 779.69; Yield 56%; m.p. 200–210 °C (decomp.). Elemental analysis, found: C: 58.31; H: 6.49; N: 7.24; S: 8.76%, calculated for C₃₈H₅₂N₄O₂S₂Sn: C: 58.54; H: 6.72; N: 7.19; S: 8.23%. IR (cm⁻¹): 3636 s, 3449 wide, 2958 s, 2874 m, 1430 s, 1401 w, 1320 m, 1239 s, 1147 m, 1122 s, 1025 w, 885 w, 864 w, 745 w, 573 w, 525 w, 382 w. ¹H-NMR (δ (ppm), DMSO d₆): 1.38 (s, 36 H, C(CH₃)₃); 2.31 s (br, 6 H, CH₃C⁴ in MPMT), 6.90 (s, 2 H, C²H in R); 7.04 (d, 2 H, ³J_{HH} = 5 Hz, C⁵H in MPMT); 7.24 (s, 2 H, ³J_{H-Sn} = 60 Hz, C²H in R); 8.32 (d, 2 H, ³J_{HH} = 5 Hz, C⁶H in MPMT). ¹³C-NMR (δ (ppm), DMSO d₆): 31.03 (C(CH₃)₃), 35.02 (CH₃C⁴ in MPMT), 35.30 (C(CH₃)₃), 116.71 (C⁵ in MPMT), 124.95 (¹J_{C-Sn} = 401 Hz, C¹ in R), 133.26 (C² in R), 139.33 (C³ in R), 154.50 (C⁴ in R), 157.42 (C⁶ in MPMT), 163.30 (C⁴ in MPMT), 180.59 (C² in MPMT).

4; R₂Sn(PYT)Cl: Mol. Wt.: 674.95; Yield 60%; m.p. 180–190 °C (decomp.). Elemental analysis, found: C: 58.10; H: 6.78; N: 1.47; S: 4.33%, calculated for C₃₃H₄₆ClNO₂SSn: C: 58.72; H: 6.87; N: 2.08; S: 4.76%. IR (cm⁻¹): 3631 s, 2959 s, 2873 m, 1708 w, 1585 w, 1429 s, 1401 w, 1362 w, 1238 m, 1203 m, 1121 m, 1001 w, 885 w, 808 w, 760 w, 727 w, 682 w, 574 w, 502 w, 375 s. ¹H-NMR (δ (ppm), CDCl₃): 1.44 (s, 36 H, C(CH₃)₃); 5.39 (s, 2 H, OH); 7.13 (dd, 1 H, ³J_{HH} = 6.5 Hz, ³J_{HH} = 6.0 Hz, C⁵H in PYT); 7.39 (d, 1 H, ³J_{HH} = 8 Hz, C³H in PYT); 7.63 (ddd, 1 H, ³J_{HH} = 8 Hz, ³J_{HH} = 6.5 Hz, ⁴J_{HH} = 1.8 Hz, C⁴H in PYT); 7.72 (s, 4H, ³J_{H-Sn} = 84 Hz, C²H in R); 8.25 (d, 1 H, ³J_{HH} = 6 Hz, C⁶H in PYT). ¹³C-NMR (δ (ppm), CDCl₃): 29.18 (C(CH₃)₃), 33.53 (C(CH₃)₃), 117.65 (C³ in PYT), 118.48 (C⁵ in PYT), 123.17 (¹J_{C-Sn} = 510 Hz, C¹ in R), 123.81 (C⁴ in PYT), 131.12 (C² in R), 135.08 (C⁴ in PYT), 137.93 (C³ in R), 145.05 (C⁴ in R), 154.72 (C² in PYT).

5; R₂Sn(mbzt)Cl: Mol. Wt.: 731.04; Yield 82%; m.p. 180 °C (decomp.). Elemental analysis, found: C: 57.49; H: 6.48; N: 1.95; S: 8.57%; calculated for C₃₅H₄₆ClNO₂S₂Sn: C: 57.50; H: 6.34; N: 1.92; S: 8.77%. IR (cm⁻¹): 3632 s, 3430 wide, 2959 s, 2874 m, 2344 m, 2362 m, 1429 s, 1402 m, 1320 m, 1240 s, 1203 w, 1121 s, 1078 w, 1036 m, 885 w, 752 m, 670 w, 571 w, 381 w. ¹H-NMR (δ (ppm), CDCl₃): 1.39 (s, 36 H, C(CH₃)₃); 5.43 (s, 2 H OH), 7.32–7.38 (m, 1 H, C⁷H in MBZT); 7.42–7.48 (m, 1 H, C⁸H in MBZT); 7.73–7.77 (m, 2 H, C⁹H, C⁶H in MBZT), 7.78 (s, 4 H, ³J_{H-Sn} = 88 Hz, C²H in R). ¹³C-NMR (δ (ppm), CDCl₃): 30.39 (C(CH₃)₃), 34.40 (C(CH₃)₃), 111.80 (C⁹ in MBZT), 119.72 (¹J_{C-Sn} = 503 Hz, C¹ in R), 121.62 (C⁶ in MBZT), 124.76 (C⁷ in MBZT), 125.02 (C² in R), 127.30 (C⁸ in MBZT), 131.95 (C⁵ in MBZT), 136.02 (C³ in R), 137.37 (C⁴ in MBZT), 153.95 (C⁴ in R), 159.38 (C² in MBZT).

Table 7 Crystal data and the structure refinement details for the complexes 1–5

	1	2	3	4	5
Empirical formula	C ₂₈ H ₄₀ Cl ₂ O ₂ Sn	C ₃₆ H ₄₈ N ₄ O ₂ S ₂ Sn	C ₃₈ H ₅₂ N ₄ O ₂ S ₂ Sn	C ₃₃ H ₄₁ ClNO ₂ SSn	C ₃₅ H ₄₄ ClNO ₂ S ₂ Sn
Fw	598.21	751.63	779.69	671.41	729.01
Temperature (K)	100(1)	100(1)	100(1)	100(1)	100(1)
Cryst. size (mm)	0.01 × 0.02 × 0.04	0.03 × 0.03 × 0.10	0.05 × 0.07 × 0.09	0.04 × 0.07 × 0.21	0.03 × 0.04 × 0.13
Cryst. system	Monoclinic	Orthorhombic	Monoclinic	Monoclinic	Monoclinic
Space group	<i>P</i> 2 ₁ / <i>c</i>	<i>C</i> 2221	<i>P</i> 2 ₁ / <i>c</i>	<i>C</i> 2/ <i>c</i>	<i>P</i> 2 ₁ / <i>n</i>
<i>a</i> (Å)	13.8030(4)	9.2953(4)	10.8406(2)	36.0304(13)	13.0191(4)
<i>b</i> (Å)	10.6301(4)	24.9586(8)	19.1873(4)	11.0367(3)	10.1141(3)
<i>c</i> (Å)	20.1254(7)	30.4963(12)	18.7686(4)	33.5317(12)	27.4822(9)
α (°)	90	90	90	90	90
β (°)	102.781(3)	90	95.944(2)	93.048(3)	102.059(3)
γ (°)	90	90	90	90	90
<i>V</i> (Å ³)	2879.78(17)	7075.1(5)	3882.91(14)	13315.2(8)	3538.90(19)
<i>Z</i>	4	8	4	8	4
ρ_{calcd} (g cm ⁻³)	1.380	1.411	1.334	1.340	1.368
μ (mm ⁻¹)	8.9	7.1	0.8	7.6	7.8
<i>R</i> , <i>wR</i> ₂ [<i>I</i> > 2 σ (<i>I</i>)], <i>S</i>	0.0835, 0.1589, 1.09	0.0329, 0.1365, 1.14	0.0357, 0.0884, 1.03	0.0505, 0.1449, 1.08	0.0381, 0.1052, 1.05

Crystallography: X-ray structure determination

Intensity data for the crystals of 1–5 were collected on an Oxford Diffraction CCD instrument, using graphite monochromated Mo radiation ($\lambda = 0.71073$ Å). Cell parameters were determined by least-squares refinement of the diffraction data from 25 reflections.^{21a}

All data were corrected for Lorentz-polarization effects and absorption.^{21a,b} The structures were solved with direct methods with SHELXS97^{21c} and refined by full-matrix least-squares procedures on *F*² with SHELXL97.^{21d} All non-hydrogen atoms were refined anisotropically, hydrogen atoms were located at calculated positions and refined *via* the “riding model” with isotropic thermal parameters fixed at 1.2 (1.3 for CH₃ groups) times the *U*_{eq} value of the appropriate carrier atom. Significant crystal data are given in Table 7.

Biological tests

These studies were performed as previously reported.¹⁸

Computational studies – theoretical methods

Eleven organotin compounds were analyzed regarding their cytotoxic activity against MCF-7 cells (Table 6) and divided into two groups according to IC₅₀ values (lower and higher than 1). Single point direct SCF calculations were carried out at the B3LYP/3-21G*/LANL2DZ(Sn) level using the Gaussian03W²² software package. Calculations were performed on the PM3 optimized molecular geometries initially derived from X-ray diffraction methods. Eleven descriptors were obtained at the DFT/polarizable continuum model (PCM) level in aqueous solutions. These included electrostatic and non-electrostatic interactions due to solvation effects and electronic structure calculations of the organotin complexes. The electrostatic term is essentially the total free energy in solution (DG(sol)) while the non-electrostatic terms include the cavitation energy (CE) based on the surface defined by the van der Waals spheres and the dispersion (DE)/repulsion (RE) energy based on the solvent's accessible surface. The total non-electrostatic term (TNE) is given by CE + DE +

RE. Evaluated electronic properties include the energy of the Kohn–Sham's frontier orbitals (HOMO and LUMO), the chemical potential (CP), global hardness (CH) and electrophilicity (EP). The three latter descriptors were calculated within the finite difference approximation and Koopman's approach²³ according to the equations CP = (HOMO + LUMO)/2, CH = (LUMO – HOMO)/2 and EP = CP²/2CH. Finally, the dipole moment (DM) was calculated as an electrostatic descriptor which efficiently explains the molecular charge distribution.

Multivariate statistical methods were employed for the analysis of the above physicochemical descriptors. PCA was performed on the produced 11 × 12 (compounds × 11 calculated descriptors plus IC₅₀) correlation matrix to effectively remove the redundancy of the original data set by compressing it into a few orthogonal uncorrelated principal components (PCs) constructed by weighted linear combinations of the original variables. These new composite variables describe most of the initial information which is actually the physicochemical properties of the complexes. The first PC explains as much of the variance as possible followed by the second one and so on. Scores are the coordinates related to PCs and loadings are the related coefficients between the original variables and the new PCs. The spatial relationship of the data is visualized by plotting a 2-dimensional score plot of the PCs in which possible clustering patterns are depicted.

Acknowledgements

The NATO grant PDD(CP)-(CBP.NR.NRCLG 983167) for the exchange of scientists is acknowledged for financial support during the visit of Dr D.S. to the University of Ioannina, Greece. The work was also supported by the Russian Foundation for Basic Research (grants No. 12-03-00776, 11-03-01165, 11-03-12088).

References

- 1 A. G. Davies, *Organotin Chemistry*, VCH, Verlagsgesellschaft, Weinheim, Germany, 1997.

- 2 M. Gielen and E. R. T. Tiekink, Tin compounds and their therapeutic potential, in *Metallotherapeutic Drugs and Metal-Based Diagnostic Agents: The Use of Metals in Medicine*, ed. M. Gielen and E. R. T. Tiekink, John Wiley & Sons, Ltd., 2005.
- 3 (a) M. Gielen, *Appl. Organomet. Chem.*, 2002, **16**, 481–494; (b) M. Gielen, M. Biesemans and R. Willem, *Appl. Organomet. Chem.*, 2005, **19**, 440–450.
- 4 S. K. Hadjikakou and N. Hadjiliadis, *Coord. Chem. Rev.*, 2009, **253**, 235–249.
- 5 A. Gennari, R. Bleumink, B. Vivani, C. L. Galli, M. Marinovich, R. Pieters and E. Corsini, *Toxicol. Appl. Pharmacol.*, 2002, **181**, 27–131.
- 6 (a) M. N. Xanthopoulou, S. K. Hadjikakou, N. Hadjiliadis, M. Kubicki, S. Karkabounas, K. Charalabopoulos, N. Kourkoumelis and T. Bakas, *J. Organomet. Chem.*, 2006, **691**, 1780–1789; (b) M. N. Xanthopoulou, S. K. Hadjikakou, N. Hadjiliadis, M. Schurmann, K. Jurkschat, A. Michaelides, S. Skoulika, T. Bakas, J. Binolis, S. Karkabounas and K. Charalabopoulos, *J. Inorg. Biochem.*, 2003, **96**, 425–434; (c) I. I. Verginadis, S. Karkabounas, Y. Simos, E. Kontargiris, S. K. Hadjikakou, A. Batistatou, A. Evangelou and K. Charalabopoulos, *Eur. J. Pharm. Sci.*, 2011, **42**, 253–261; (d) M. N. Xanthopoulou, S. K. Hadjikakou, N. Hadjiliadis, M. Kubicki, S. Skoulika, T. Bakas, M. Baril and I. S. Butler, *Inorg. Chem.*, 2007, **46**, 1187–1195.
- 7 (a) V. I. Balas, I. I. Verginadis, G. D. Geromichalos, N. Kourkoumelis, L. Male, M. B. Hursthouse, K. H. Repana, E. Yiannaki, K. Charalabopoulos, T. Bakas and S. K. Hadjikakou, *Eur. J. Med. Chem.*, 2011, **46**, 2835–2844; (b) V. I. Balas, S. K. Hadjikakou, N. Hadjiliadis, N. Kourkoumelis, M. E. Light, M. Hursthouse, A. K. Metsios and S. Karkabounas, *Bioinorg. Chem. Appl.*, 2008, Article ID 654137.
- 8 A. Szorcik, L. Nagy, M. Scopelliti, A. Deak, L. Pellerito and K. Hegetschweiler, *J. Organomet. Chem.*, 2005, **690**, 2243–2253.
- 9 (a) D. M. Parkin, F. Bray, J. Ferlay and P. Pisani, *CA Cancer J. Clin.*, 2005, **55**, 74–108; (b) S. Leporatti, D. Vergara, A. Zacheo, V. Vergaro, G. Maruccio, R. Cingolani and R. Rinaldi, *Nanotechnology*, 2009, **20**, 055103; (c) N. Kobakhidze, N. Farfan, M. Romero, J. M. Mendez-Stivale, M. G. Ballinas-Lopez, H. Garcia-Ortega, O. Dominguez, R. Santillan, F. Sanchez-Bartez and I. Gracia-Mora, *J. Organomet. Chem.*, 2010, **695**, 1189–1199; (d) A. W. Norman, M. T. Mizwicki and D. P. G. Norman, *Nat. Rev. Drug Discovery*, 2004, **3**, 27–41; (e) A. S. Levenson and V. C. Jordan, *Cancer Res.*, 1997, **57**, 3071–3078; (f) M. Razandi, A. Pedram and E. R. Levin, *Mol. Endocrinol.*, 2000, **14**, 1434–1447.
- 10 E. Denisov, *Handbook of Antioxidants*, CRC Press, Boca Raton, USA, 1995.
- 11 (a) E. R. Milaeva, S. I. Filimonova, N. N. Meleshonkova, L. G. Dubova, E. F. Shevtsova, S. O. Bachurin and N. S. Zefirov, *Bioinorg. Chem. Appl.*, 2010, DOI: 10.1155/2010/165482, Article ID 165482; (b) E. R. Milaeva, Yu. A. Gracheva, D. B. Shpakovsky, O. A. Gerasimova, V. Yu. Tyurin and V. S. Petrosyan, *J. Porphyrins Phthalocyanines*, 2003, **7**, 719–724; (c) E. R. Milaeva, V. Yu. Tyurin, D. B. Shpakovsky, O. A. Gerasimova, Z. Jingwei and Yu. A. Gracheva, *Heteroat. Chem.*, 2006, **17**, 475–480; (d) E. R. Milaeva, O. A. Gerasimova, Z. Jingwei, D. B. Shpakovsky, S. A. Syrbu, A. S. Semeykin, O. I. Koifman, E. G. Kireeva, E. F. Shevtsova, S. O. Bachurin and N. S. Zefirov, *J. Inorg. Biochem.*, 2008, **102**, 1348–1358; (e) E. R. Milaeva, V. Yu. Tyurin, Yu. A. Gracheva, M. A. Dodochova, L. M. Pustovalova and V. N. Chernyshev, *Bioinorg. Chem. Appl.*, 2006, DOI: 10.1155/bca/2006/64927, Article ID64927.
- 12 A. G. Milaev and O. Yu. Okhlobystin, *Russ. J. Gen. Chem.*, 1978, **48**, 1186.
- 13 K. C. Molloy, T. G. Purcell, D. Cunningham, P. McCardle and T. Higgins, *Appl. Organomet. Chem.*, 1987, **1**, 119–131.
- 14 (a) P. J. Smith, *Chemistry of Tin*, Blackie Academic & Professional an imprint of Thomson Science, London UK, 1998; (b) R. Schmiedgen, F. Huber, A. Silvestri, G. Ruisi, M. Rossi and R. Barbieri, *Appl. Organomet. Chem.*, 1998, **12**, 861–871; (c) R. V. Parish, In *Mossbauer Spectroscopy Applied to Inorganic Chemistry*, ed. G.J. Long, Plenum Press, New York, 1984; (d) G. M. Bancroft and R. H. Platt, *Adv. Inorg. Chem. Radiochem.*, 1972, **15**, 59–133.
- 15 (a) S. Mahmood, S. Ali, M. H. Bhatti, M. Mazhar and K. Shahid, *Turk. J. Chem.*, 2004, **28**, 17–26; (b) P. C. Srivastava, A. Trivedi and P. Singh, *Polyhedron*, 1990, **1**, 125–128; (c) I. A. Portnyagin, V. V. Lunin and M. S. Nechaev, *J. Organomet. Chem.*, 2008, **693**, 3847–3850; (d) N. N. Meleshonkova, D. B. Shpakovsky, A. V. Fionov, A. V. Dolganov, T. V. Magdesieva and E. R. Milaeva, *J. Organomet. Chem.*, 2007, **692**, 5339–5344; (e) T. P. Lockhart, W. F. Manders and J. J. Zuckerman, *J. Am. Chem. Soc.*, 1985, **107**, 4546; (f) W. Rehman, K. M-Baloch and A. Badshah, *Eur. J. Med. Chem.*, 2008, **43**, 2380–2385; (g) W. Rehman, A. Badshah, S. Khan and L.-T.-A. Tuyet, *Eur. J. Med. Chem.*, 2009, **44**, 3981–3985.
- 16 A. G. Milaev, V. B. Panov and O. Yu. Okhlobystin, *J. Gen. Chem.*, 1978, **48**, 2715–2720.
- 17 (a) A. W. Addison, T. Nageswara Rao, J. Reedijk, J. Van Rijn and G. C. Verschoor, *J. Chem. Soc., Dalton Trans.*, 1984, 1349–1356; (b) D. F. Shiver, P. W. Atkins and C. H. Langford, in *Inorganic Chemistry*, 3rd edn, Oxford University Press, Oxford, U.K., 1999.
- 18 C. N. Banti, A. D. Giannoulis, N. Kourkoumelis, A. M. Owczarzak, M. Poyraz, M. Kubicki, K. Charalabopoulos and S. K. Hadjikakou, *Metallomics*, 2012, **4**, 545–560.
- 19 (a) C. Ma and J. Zhang, *Appl. Organomet. Chem.*, 2003, **17**, 788–794; (b) M. N. Xanthopoulou, S. K. Hadjikakou, N. Hadjiliadis, N. Kourkoumelis, E. R. Milaeva, J. A. Gracheva, V.-Y. Tyurin, I. I. Verginadis, S. Karkabounas, M. Baril and I. S. Butler, *Russ. Chem. Bull.*, 2007, **56**, 767–773; (c) M. N. Xanthopoulou, S. K. Hadjikakou, N. Hadjiliadis, E. R. Milaeva, J. A. Gracheva, V.-Y. Tyurin, N. Kourkoumelis, K. C. Christoforidis, A. K. Metsios, S. Karkabounas and K. Charalabopoulos, *Eur. J. Med. Chem.*, 2008, **43**, 327–335.
- 20 A. K. Saxena and F. Huber, *Coord. Chem. Rev.*, 1989, **95**, 109–123.
- 21 (a) CrysAlis RED, version 1.171.31.5; Oxford Diffraction Ltd. (release 28–08–2006 CrysAlis171.NET); (b) Oxford Diffraction, CRYSA LIS CCD and CRYSA LIS RED, version p171.29.2; Oxford Diffraction Ltd: Abingdon, Oxford, England, 2006; (c) G. M. Sheldrick, *Acta Crystallogr., Sect. A: Fundam. Crystallogr.*, 1990, **46**, 467; (d) G. M. Sheldrick, *Acta Crystallogr., Sect. A: Fundam. Crystallogr.*, 2008, **64**, 112–122.
- 22 M. J. Frisch, G. W. Trucks, H. B. Schlegel, G. E. Scuseria, M. A. Robb, J. R. Cheeseman, J. A. Montgomery Jr, T. Vreven, K. N. Kudin, J. C. Burant, J. M. Millam, S. S. Iyengar, J. Tomasi, V. Barone, B. Mennucci, M. Cossi, G. Scalmani, N. Rega, G. A. Petersson, H. Nakatsuji, M. Hada, M. Ehara, K. Toyota, R. Fukuda, J. Hasegawa, M. Ishida, T. Nakajima, Y. Honda, O. Kitao, H. Nakai, M. Klene, X. Li, J. E. Knox, H. P. Hratchian, J. B. Cross, V. Bakken, C. Adamo, J. Jaramillo, R. Gomperts, R. E. Stratmann, O. Yazyev, A. J. Austin, R. Cammi, C. Pomelli, J. W. Ochterski, P. Y. Ayala, K. Morokuma, G. A. Voth, P. Salvador, J. J. Dannenberg, V. G. Zakrzewski, S. Dapprich, A. D. Daniels, M. C. Strain, O. Farkas, D. K. Malick, A. D. Rabuck, K. Raghavachari, J. B. Foresman, J. V. Ortiz, Q. Cui, A. G. Baboul, S. Clifford, J. Cioslowski, B. B. Stefanov, G. Liu, A. Liashenko, P. Piskorz, I. Komaromi, R. L. Martin, D. J. Fox, T. Keith, M. A. Al-Laham, C. Y. Peng, A. Nanayakkara, M. Challacombe, P. M. W. Gill, B. Johnson, W. Chen, M. W. Wong, C. Gonzalez and J. A. Pople, *GAUSSIAN 03 (Revision C.02)*, Gaussian, Inc., Wallingford CT, 2004.
- 23 P. Geerlings, F. De Prof and W. Langenaeker, Conceptual density functional theory, *Chem. Rev.*, 2003, **103**, 1793–1874.